## Microscopic Study of the Superconducting State of the Iron Pnictide RbFe<sub>2</sub>As<sub>2</sub>

Z. Shermadini,<sup>1,2</sup> J. Kanter,<sup>3</sup> C. Baines,<sup>1</sup> M. Bendele,<sup>1,4</sup> Z. Bukowski,<sup>3</sup> R. Khasanov,<sup>1</sup> H.-H. Klauss,<sup>2</sup> H. Luetkens,<sup>1</sup> H. Maeter,<sup>2</sup> G. Pascua,<sup>1</sup> B. Batlogg,<sup>3</sup> and A. Amato<sup>1</sup>

<sup>1</sup>Laboratory for Muon Spin Spectroscopy, Paul Scherrer Institute, CH-5232 Villigen PSI, Switzerland
<sup>2</sup>Institut für Festkörperphysik, TU Dresden, D-01069 Dresden, Germany
<sup>3</sup>Laboratory for Solid State Physics, ETH Zürich, CH-8093 Zürich, Switzerland
<sup>4</sup>Physik-Institut der Universität Zürich, Winterthurerstrasse 190, CH-8057 Zürich, Switzerland

A study of the temperature and field dependence of the penetration depth  $\lambda$  of the superconductor RbFe<sub>2</sub>As<sub>2</sub> ( $T_c=2.52$  K) was carried out by means of muon-spin rotation measurements. In addition to the zero temperature value of the penetration depth  $\lambda(0)=267(5)$  nm, a determination of the upper critical field  $B_{c2}(0)=2.6(2)$  T was obtained. The temperature dependence of the superconducting carrier concentration is discussed within the framework of a multi-gap scenario. Compared to the other "122" systems which exhibit much higher Fermi level, a strong reduction of the large gap BCS ratio  $2\Delta/k_{\rm B}T_c$  is observed. This is interpreted as a consequence of the absence of interband processes. Indications of possible pair-breaking effect are also discussed.

The iron arsenide AFe<sub>2</sub>As<sub>2</sub> systems (where A is an alkaline earth element) crystallize with the tetragonal Th $Cr_2Si_2$  type structure (space group I4/mmm)<sup>1</sup>. The interest for these compounds arises from the observation of superconductivity with transition temperatures  $T_c$  up to 38 K upon alkali metal substitution for the A element<sup>2-4</sup>, or partial transition metal substitution for iron<sup>5</sup>. A huge number of studies were already devoted to unravel the properties of their superconducting ground state. However, some studies are hampered by the fact that to date no clear picture could be drawn about the bulk character of the superconductivity. For example, in superconducting systems obtained from the substitution of the A element (like K for Ba), muon-spin rotation/relaxation ( $\mu$ SR) measurements studies clearly indicate the occurrence of phase separation between magnetic and superconducting phases 6-8. On the other hand, substitution performed on the superconducting plane, as cobalt substitution for iron, does not reveal any phase separation as reported also by  $\mu SR^9$ .

The alkali metal iron arsenide RbFe<sub>2</sub>As<sub>2</sub> was discovered some years ago<sup>10</sup> but was only recently found, by Bukowski et al.<sup>11</sup>, to exhibit type II bulk superconductivity below  $T_c \simeq 2.6$  K. The reported studies were hindered by a limited temperature range of the equipment and the full development of the Meissner state could not be recorded. The estimated value of the upper critical field at zero temperature,  $B_{c2} \simeq 2.5$  T, was obtained from magnetization measurements performed at various field down to 1.5 K in the mixed state and by assuming a temperature dependence provided by the Werthamer–Helfand–Hohenberg theory<sup>11</sup>.

Compared to the better known compound  $BaFe_2As_2$ ,  $RbFe_2As_2$  possesses a lower Fermi level and is characterized by the absence of magnetic instability. Furthermore, the electron deficiency in  $RbFe_2As_2$  leads also to a change (i.e. a decrease) of the number of bands contributing to the superconducting state, compared for example to  $Ba_{1-x}K_xFe_2As_2$ . Hence, one expects a strong decrease of the contribution of the electron-like bands at the M

point of the Fermi surface. Such a decrease has been observed by angle-resolved photoemission spectroscopy  $^{12}$  in the analog system KFe<sub>2</sub>As<sub>2</sub>, which also presents a case of naturally hole-(over)doped system when compared to the alkaline earth "122" iron-based superconductors.

As exemplified by a number of recent studies, the  $\mu$ SR technique is very well suited to investigate the superconducting properties of iron-based systems (see for example Ref. 13). In addition, due to its comparatively low upper critical field  $B_{c2}$  and its reduced  $T_c$ , the system RbFe<sub>2</sub>As<sub>2</sub> opens a unique opportunity to fully study the B-T phase diagram of an iron-arsenide compound.

In this article, we report on a detailed study of the temperature and field dependence of the magnetic penetration depth of RbFe<sub>2</sub>As<sub>2</sub>, which is closely related to the superconducting carrier concentration.

Polycrystalline samples of RbFe<sub>2</sub>As<sub>2</sub> were synthesized in two steps as reported recently<sup>11</sup>. The  $\mu$ SR measurements were performed at the  $\pi$ M3 beamline of the Paul Scherrer Institute (Villigen, Switzerland), using the GPS instrument (for temperatures down to 1.6 K and field up to 0.6 T) as well as the LTF instrument (for temperatures down to 0.02 K and higher fields). Both zero field (ZF) and transverse field (TF)  $\mu$ SR measurements were performed. Additional transport studies were performed on the very same sample at the ETH-Zürich using an ac Transport Option of a Quantum Design 14T-PPMS.

To exclude the occurrence of any magnetic contributions of the Fe ions at low temperature, we performed first ZF mesurements above and below  $T_c$ . As exemplified by the data reported on Fig. 1a, no sign of static magnetism could be detected on the ZF response RbFe<sub>2</sub>As<sub>2</sub>. The data are well described by a standard Kubo-Toyabe depolarization function<sup>14</sup>, reflecting the field distribution at the muon site created by the nuclear moments. The marginal increase of the depolarization rate, not related to the superconducting transition, possibly points to a slowing down of the magnetic fluctuations.

Figure 1b exhibits the TF  $\mu$ SR time spectra measured in an applied field of 0.01 T, above (T=4 K) and be-

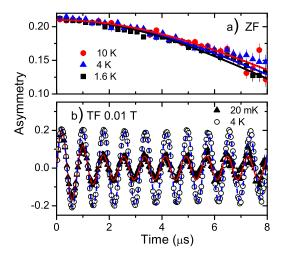


FIG. 1: Typical  $\mu$ SR spectra recorded above and below  $T_c$ , in: a) zero field; and b) transverse field.

low  $(T=0.02~{\rm K})$  the superconducting transition temperature. The strong muon-spin depolarization at low temperatures reflects the formation of the flux-line lattice (FLL) in the superconducting state. The long-lived component detectable at low temperatures is due to a background contribution from the sample holder. In a polycrystalline sample the magnetic penetration depth  $\lambda$  (and consequently the superconducting carrier concentration  $n_{\rm s} \propto 1/\lambda^2$ ) can be extracted from the Gaussian muon-spin depolarization rate  $\sigma_{\rm s}(T)$  (see also below Eq. 2), which reflects the second moment  $(\sigma_{\rm s}^2/\gamma_{\mu}^2)$  of the magnetic field distribution due to the FLL in the mixed state. The TF data were analyzed using the polarization function:

$$A_0 P(t) = A_{\rm s} \exp\left[-\frac{(\sigma_{\rm s}^2 + \sigma_{\rm n}^2)t^2}{2}\right] \cos(\gamma_{\mu} B_{\rm int} t + \varphi)$$
$$+A_{\rm sh} \exp(-\frac{\sigma_{\rm sh}^2 t^2}{2}) \cos(\gamma_{\mu} B_{\rm sh} t + \varphi) . \quad (1)$$

The first term on the right-hand side of Eq. 1 represents the sample contribution, where  $A_{\rm s}$  denotes the initial asymmetry connected to the sample signal;  $\sigma_{\rm s}$  is the Gaussian relaxation rate due to the FLL;  $\sigma_{\rm n}$  is the contribution to the field distribution arising from the nuclear moment and which is found to be temperature independent, in agreement with the ZF results;  $B_{\rm int}$  is the internal magnetic field, sensed by the muons and  $\varphi$  is the initial phase of the muon-spin ensemble. The second term reflects the muons stopping in the silver sample holder, where  $A_{\rm sh}$  denotes the initial asymmetry connected to the holder signal;  $\sigma_{\rm sh}$  is the relaxation rate due to the nuclear moments (which is very close to zero in this case) and  $B_{\rm sh}$  is the magnetic field in the sample holder, which has essentially the value of the external field.

On Fig. 2, we report the temperature dependence of  $\sigma_{\rm s}$  extracted from TF- $\mu$ SR measurements in four different fields. We note first that the perfect fits obtained by assuming a Gaussian field distribution of the FLL

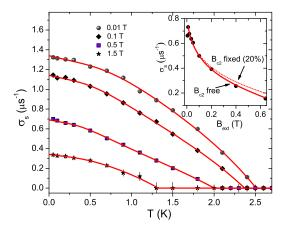


FIG. 2: Temperature dependence of the depolarization rate due to the FLL in RbFe<sub>2</sub>As<sub>2</sub> and obtained in fields of 1.5, 0.5, 0.1 and 0.01 T (lines are guides to the eye). Insert: Field dependence of  $\sigma_{\rm s}$  obtained at 1.6 K and analyzed using the Eq. 2. The dashed line represents a fit using the  $B_{c2}$  value given by the magnetoresistivity data (with an arbitrary criterium of a resistivity increase corresponding to 20% of its value in the normal state). The solid line corresponds to a similar analysis, but considering  $B_{c2}$  as a free parameter.

point to a rather large anisotropy of the magnetic penetration depth in our system. This is confirmed by recent  $\mu$ SR measurements performed on hole- and electrondoped "122" systems<sup>8,9</sup>. As expected,  $\sigma_s$  is zero in the paramagnetic state and starts to increase below  $T_c(B)$ when the FLL is formed. Upon lowering the temperature,  $\sigma_{\rm s}$  increases gradually reflecting the decrease of the penetration depth or, alternatively, the increase of the superconducting density. The overall decrease of  $\sigma_s$  at very low temperatures observed upon increasing the applied field is a direct consequence of the decrease of the width of the internal field distribution when increasing the field towards  $B_{c2}$ . In order to quantify such an effect, one can make use of the numerical Ginzburg-Landau model, developed by  $Brandt^{15}$ . This model allows one to calculate the superconducting carrier concentration with good approximation within the local (London) approximation  $(\lambda \gg \xi, \xi)$  is the coherence length). This model predicts the magnetic field dependence of the second moment of the magnetic field distribution or, alternatively, of the  $\mu SR$  depolarization rate, which can be expressed

$$\sigma_{\rm s} \left[ \mu {\rm s}^{-1} \right] = 4.83 \times 10^4 (1 - B/B_{c2}) \times \left[ 1 + 1.21 (1 - \sqrt{B/B_{c2}})^3 \right] \lambda^{-2} \left[ {\rm nm} \right]$$
 (2)

The insert of Fig. 2 exhibits the evolution of  $\sigma_{\rm s}$  at 1.6 K as a function of the external applied magnetic field. For each data point, the sample was field-cooled from above  $T_c$  down to 1.6 K and the recorded  $\mu{\rm SR}$  spectra were analyzed with Eq. 1. The field dependence of  $\sigma_{\rm s}$  was analyzed with Eq. 2 using the values of the upper critical field  $B_{c2}$  given either by an arbitrary criterium based on magnetoresistivity measurements (see Fig. 3a) or by leav-

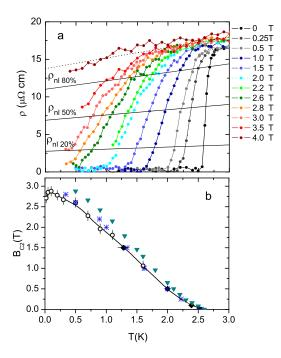


FIG. 3: a) Field dependence of the electrical resistivity. b) Upper critical field for RbFe<sub>2</sub>As<sub>2</sub>. The open circles are obtained by analyzing the field dependence of  $\sigma_{\rm s}$  using Eq. 2, as explained in the text. The diamonds are the value obtained by analyzing the temperature dependence of  $\sigma_{\rm s}$ . The blue stars correspond to the complete disappearence of the resistivity in field. For comparison, we report the values given by the magnetoresistivity data with the same criterium used in the insert of Fig. 2 and corresponding to the values extracted along the line  $\rho_{\rm nl~20\%}$  of the upper panel. The line is a guide to the eye.

ing the parameter  $B_{c2}$  free. The latter option provides excellent fits for all temperatures and the corresponding fitted values of the superconducting carrier concentration and of the upper critical fields are reported on Fig. 4 and 3b. An additional point provided by this first investigation, is that the penetration depth can be assumed to be field independent. This rules out the possibility that RbFe<sub>2</sub>As<sub>2</sub> is a nodal superconductor, since a field should have induced excitations at the gap nodes due to nonlocal and nonlinear effects, thus reducing the superconducting carrier concentration  $n_{\rm s}$  and therefore affecting  $\lambda$  (see for example Ref. 16).

By looking at the temperature dependence of  $\lambda^{-2}$  obtained using Eq. 2 with the values of the parameter  $B_{c2}(T)$  presented on Fig. 3b, the zero-temperature value of the penetration depth  $\lambda(0) = 267(5)$  nm can be deduced. The obtained temperature dependence of  $\lambda^{-2}$  was analyzed, in a first step, within the framework of a BCS single s-wave symmetry superconducting gap  $\Delta$  (see Fig. 4), using the form<sup>17</sup>:

$$\frac{\lambda^{-2}(T)}{\lambda^{-2}(0)} = 1 - \frac{2}{k_B T} \int_{\Delta}^{\infty} f(\epsilon, T) \left[ 1 - f(\epsilon, T) \right] d\epsilon , \quad (3)$$

where  $f(\epsilon, T) = (1 + \exp[\sqrt{\epsilon^2 + \Delta(T)^2}/k_B T])^{-1}$ , and with a standard BCS temperature dependence for the

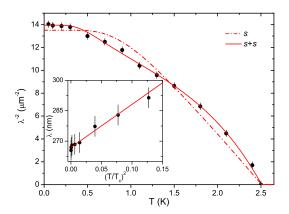


FIG. 4: Magnetic penetration depth as a function of temperature. Above 0.5 K, the values obtained with Eq. 2 coincides with the values measured in a field of 0.01 T, and only these latter are plotted for this temperature range. The red dashed line corresponds to a BCS s-wave gap symmetry, whereas the solid one to represents a fit using a two-gap s + s model. The insert exhibits the penetration depth as a function of  $(T/T_c)^2$ .

gap function. As evidenced on Fig. 4, this analysis is not satisfactory. We note also that a d-wave symmetry model does not fit the data, confirming at posteriori the discussion of a field independent penetration depth. These results are actually not unexpected, as there are growing evidences that several disconnected Fermi-surface sheets contribute to the superconductivity, as revealed by angleresolved photoemission spectroscopy<sup>12</sup>, resulting into two distinct values of superconducting gaps. Hence, in a second step, the experimental  $\lambda^{-2}(T)$  data were analyzed by assuming two independent contributions with different values  $\Delta_i$  of s-wave gaps<sup>8,18,19</sup>. On Fig. 4 the solid line shows a s+s multi-gap function which fits to the experimental data rather well. The parameters extracted from the fit are  $\Delta_1(0) = 0.15(2)$  meV for the small gap value (contributing  $\omega = 36\%$  to the total amount of  $n_s$ ) and  $\Delta_2 = 0.49(4)$  meV for the larger one. However, note that according to Eq. 3,  $\lambda^{-2}$  is insensitive to the phase of the superconducting gap(s). By considering the intrinsic hole-doping in RbFe<sub>2</sub>As<sub>2</sub> compared to the optimally doped "122" iron-based system, it is natural to consider that the gaps values are connected respectively to the outer  $(\beta)$  and inner  $(\alpha)$  hole-like bands at the Γ point of the Fermi surface. In this frame, RbFe<sub>2</sub>As<sub>2</sub> can be considered as hole-overdoped with electron-like  $\gamma$ and  $\delta$  bands at the M point, which shift to the unoccupied side. Note that in optimally doped "122" systems, one observes the occurrence of  $\epsilon$  hole bands (so-called "blades") around the M point, which also slightly contribute to the superconducting carrier concentration.

An additional support for a two-gap superconducting state could be provided by the observed positive curvature of the  $B_{c2}(T)$  near  $T_c$ , in sharp contrast to the usual  $B_{c2}$  BCS temperature dependence (see Fig. 3b). Note first that the values of  $B_{c2}$  extracted from the fit with Eq. 2 are in perfect agreement with: i) the values corresponding to the complete suppression of the elec-

trical resistivity in field; and ii) to the values obtained by analyzing the temperature dependence of  $\sigma_s$  in different magnetic fields (see Fig. 2). An additional indication that bulk superconductivity occurs when the electrical resistivity completely vanishes is provided by specific heat measurements<sup>20</sup> performed in zero-applied field for which the observed  $T_c$  corresponds to 2.50(1) K.

Similar positive curvature of the  $B_{c2}(T)$  near  $T_c$  were observed in  $\mathrm{MgB_2}^{21,22}$  and in the borocarbides<sup>23</sup>, where it was explained within a two-gap model. However, one should keep in mind that alternative explanations for the observed positive curvature in  $B_{c2}(T)$  are possible and that complementary measurements, as here our  $\lambda^{-2}(T)$  data, are necessary to draw conclusions.

If on one hand, the two-gap model scenario appears to best fit the temperature dependence of the penetration depth, on the other hand one could argue that it does not appear fully consistent with the observation that the field evolution of the field distribution follows Eq. 2. Hence for a two-gap model, one expects a deviation from the simple field dependence reflecting the occurrence of distinct lengths scales  $\xi_i$  for both gaps (associated to the coherence length, for a clean single gap system). Such behavior is for example clearly observed on the archetypical twogap superconductor MgB<sub>2</sub><sup>24</sup>. The experimental observation that Eq. 2 reproduces our data indicates a small difference between the  $\xi_i$  parameters for both bands. This is also inline with the very good agreement between the extracted values of  $B_{c2}$  with Eq. 2 and the observed values by resistivity. In this frame, we also mention that ARPES measurements<sup>25</sup> on members of the "122" family indicate that the Fermi velocity of the inner  $\Gamma$ -barrel band ( $\alpha$  band) is substantially higher that the one for the outer  $\Gamma$ -barrel band ( $\beta$  band), which therefore weakens the difference of the gap values on the  $\xi_i$  parameters (as  $\xi \propto \langle v_{\rm F} \rangle / \Delta$ ). Finally, we note that the observed depolarization rate in RbFe<sub>2</sub>As<sub>2</sub> is about 40 times weaker than the one reported for MgB<sub>2</sub>, hampering therefore the determination of possible distinct  $\xi_i$  length scales.

For completeness, we discuss now the slight deviation observed at very low temperatures from the s+s fit and the  $\lambda^{-2}(T)$  data. Recently, it was shown that the observation of universal scalings in the whole iron-pnictides superconductors, for the specific heat jump  $(\Delta C \propto T_c^3)$  and the slope of upper critical field at  $T_c$   $(dB_{c2}/dT \propto T_c)$  could be interpreted as signatures for strong pair-breaking effects<sup>26</sup>, as for example magnetic scattering. In the same frame it was deduced<sup>27</sup> that such

an effect should lead to a very low temperature dependence of the penetration depth deviating from an usual exponential behavior and transforming into a quadratic one, i.e.  $\lambda \propto T^2$ , which is indeed reported in a number of studies (see for example Ref. 28,29). On the insert of Fig. 4 we report the extracted penetration depth as a function of  $(T/T_c)^2$ . The good scaling is inline with the presence of magnetic scattering in RbFe<sub>2</sub>As<sub>2</sub>, as previously reported for hole- or electron-doped "122" systems<sup>27</sup>.

To conclude,  $\mu SR$  measurements were performed on a RbFe<sub>2</sub>As<sub>2</sub> polycrystalline sample. From the temperature and field dependence of the superconducting response of the  $\mu SR$  signal, the values of the upper critical field and of the magnetic penetration depth could be extracted. The zero temperature values of  $B_{c2}(0)$  and  $\lambda(0)$  were estimated to be 2.6(2) T and 267(5) nm, respectively. The temperature dependence of the penetration depth, and similarly of the superconducting carrier concentration, are reproduced assuming a multi-gap model, with possibly pair-breaking effects at low temperatures. The multi-gap scenario is supported by the observation of a clear positive curvature on the temperature dependence of the upper critical field. We attribute these gaps to the hole-like bands around the  $\Gamma$  point of the Fermi surface, and possibly also to the hole-bands blades around the M point. Assuming that the  $\gamma$  and  $\delta$  electron-like bands around the M point are in the unoccupied side, one would expect an absence of nesting conditions in RbFe<sub>2</sub>As<sub>2</sub>. The consequence would be an absence of magnetic order, as confirmed by our ZF data, and a strong decrease of the interband processes between the  $\alpha$  and  $\gamma(\delta)$  bands. In this frame, it is remarkable to see that the ratio between the gaps values is decreased by a factor more than 2 compared to optimally doped "122" systems. Similarly, we note that the BCS ratio  $2\Delta/k_{\rm B}T_c$  for the small gap that we assign to the  $\beta$  band is almost identical to the values observed for optimally doped  $Ba_{1-x}K_xFe_2As_2$ , i.e.  $2\Delta_1/k_{\rm B}T_c\simeq 1.4$ . On the other side, for the large gap of the  $\alpha$  band, this ratio is strongly reduced<sup>8,25</sup>, confirming therefore the possible role played by interband processes in optimally hole-doped iron-based "122" superconduc-

Part of this work was performed at the Swiss Muon Source (S $\mu$ S), Paul Scherrer Institute (PSI, Switzerland). The work of M.B. was supported by the Swiss National Science Foundation. The work at the IFW Dresden has been supported by the DFG through FOR 538.

<sup>&</sup>lt;sup>1</sup> M. Pfisterer and G. Nagorsen, Z. Naturforsch. **35** (1980).

<sup>&</sup>lt;sup>2</sup> M. Rotter et al., Phys. Rev. Lett. **101**, 107006 (2008).

<sup>&</sup>lt;sup>3</sup> K. Sasmal et al., Phys. Rev. Lett. **101**, 107007 (2008).

<sup>&</sup>lt;sup>4</sup> Z. Bukowski et al., Phys. Rev. B **79**, 104521 (2009).

<sup>&</sup>lt;sup>5</sup> A. S. Sefat et al., Phys. Rev. Lett. **101**, 117004 (2008).

<sup>&</sup>lt;sup>6</sup> A. A. Aczel et al., Phys. Rev. B **78**, 214503 (2008).

<sup>&</sup>lt;sup>7</sup> J. T. Park et al., Phys. Rev. Lett. **102**, 117006 (2009).

<sup>&</sup>lt;sup>8</sup> R. Khasanov et al., Phys. Rev. Lett. **102**, 187005 (2009).

<sup>&</sup>lt;sup>9</sup> R. Khasanov et al., Phys. Rev. Lett. **103**, 067010 (2009).

<sup>&</sup>lt;sup>10</sup> A. Czybulka et al., Z. Anorg. Allg. Chem. **122**, 609 (1992).

 $<sup>^{11}\,</sup>$  Z. Bukowski et al., arXiv:0909.2740v1 (2009).

<sup>&</sup>lt;sup>12</sup> T. Sato et al., Phys. Rev. Lett. **103**, 047002 (2009).

<sup>&</sup>lt;sup>13</sup> A. Amato et al., Physica. C **469**, 606 (2009).

<sup>&</sup>lt;sup>14</sup> R. Kubo and T. Toyabe, Magnetic Resonance and Relax-

- ation (North Holland, Amsterdam, 1967).
- E. H. Brandt, Phys. Rev. B 68, 054506 (2003).
   M. Amin et al., Phys. Rev. Lett. 84, 5864 (2000).
- $^{\rm 17}$  M. Tinkham,  $Introduction\ to\ Superconductivity$  (McGraw-Hill Inc., 1996).
- <sup>18</sup> C. Niedermayer et al., Phys. Rev. B **65**, 094512 (2002).
- <sup>19</sup> A. Carrington and F. Manzano, Physica C **385**, 205 (2003).

- A. Carrington and F. Manzano, Fingsice 5 305, 255 (2002).
   J. Kanter, private communication.
   O. de Lima et al., Phys. Rev. Lett. 86, 5974 (2001).
   A. Sologubenko et al., Phys. Rev. B 65, 180505 (2002).
- $^{23}\,$  S. Shulga et al., Phys. Rev. Lett.  ${\bf 80},\,1730$  (1998).
- S. Serventi et al., Phys. Rev. Lett. 93, 217003 (2004).
   D. V. Evtushinsky et al., New J. Phys. 11, 180409(R) (2010).

- <sup>26</sup> V. G. Kogan, Phys. Rev. B **80**, 214532 (2009).

  <sup>27</sup> R. T. Gordon et al., arXiv:0912.5346 (2010).

  <sup>28</sup> C. Martin et al., Phys. Rev. Lett. **102**, 247002 (2010).

  <sup>29</sup> H. Kim et al., arXiv:1001.2042v1 (2010).